

Cite this: *Mater. Horiz.*, 2020,
7, 3005Received 27th July 2020,
Accepted 3rd September 2020

DOI: 10.1039/d0mh01200a

rsc.li/materials-horizons

Photo-induced crystallization with emission enhancement (PICEE)[†]

Kongqi Chen,^a Rongyuan Zhang,^b Ganggang Li,^a Baoxi Li,^a Yao Ma,^a Ming Sun,^{id a}
Zhiming Wang^{id *ac} and Ben Zhong Tang^{id *acd}

Compared to the universal photochemical mechanism in photo-activation, the photophysical-dominant behavior is rarely reported. In this study, a luminogen with aggregation-induced emission characteristic named TIOdB with a double-ionized framework was prepared, and it exhibited an obvious photoactivation phenomenon with continuous light irradiation. Employing a series of spectral and electro experiments, the morphology and crystal analyses, and theoretical simulation, the potential mechanism of photo-induced crystallization with emission enhancement (PICEE) is presented to illuminate this photoactivation process, which offered a novel strategy for the *in situ* formation of nanocrystals. Particularly, the linear relationship between the illumination intensity and fluorescence enhancement of TIOdB was revealed, which has the potential to optimize plant growth conditions. Besides, TIOdB could be used as a high-quality mitochondrion imaging probe with the light-activated property and cancer cell killing performance.

Introduction

Light, as a significantly clean energy with no waste generation, plays an indispensable role in the development of human civilization.¹ It is vital for the photosynthesis process in which green plants assimilate carbon dioxide (CO₂) and water (H₂O) to produce organic substances and release oxygen.² Since artificial

New concepts

The common photoactivatable behaviours are usually caused by photochemical processes and require energy consumption, causing additional inconvenience and environmental issues. In comparison, the photophysical process can be easily controlled and more environmentally proceeded. Herein, TIOdB, an isoquinolinium-based organic salt derivative, was prepared to be an ionic-type AIEgen employing the tetraphenyl ethylene (TPE) framework, exhibiting an excellent photoactivatable behaviour with a new photophysical-dominant mechanism. Such a mechanism, photo-induced crystallization with emission enhancement (PICEE), was elucidated by a series of spectral and electro experiments, morphology and crystal analysis, and theoretical simulation. Moreover, this process offered a novel strategy for the *in situ* formation of nanocrystals. Owing to TIOdB excellent characteristics, it could be used as a high-quality mitochondrion imaging probe with light activated characteristic, generation ability of reactive oxygen species (ROS) and photodynamic therapy (PDT) performance. All of these indicate that it can provide a new general and simple strategy for the formation of nanocrystals, and under the guidance of such new photoactivatable mechanism, diverse functional materials can be developed in practical life.

functional materials related to light (generation, storage and conversion) have been attracting continuous attention and bringing about great advances to our life, research on photo-response materials have been widely investigated in science history in materials operation, such as photothermal, photovoltaics and optical memories.^{3–5}

Recently, the photoactivatable materials have attracted increasing interest due to their potential applications in super-resolution imaging,⁶ biosensing,⁷ and optical switch related areas.⁸ However, the common photoactivatable behaviour is usually caused by photochemical processes such as photoreaction, photocyclization, and photoisomerization,⁹ most of which work between two or more stable states and require energy consumption, imposing additional inconvenience.¹⁰ Moreover, such mechanism of photochemical conversion may severely impede the development of materials with new optoelectronic properties. In comparison, the photophysical process can be easily controlled and is more environmentally friendly. For example, aggregation-induced emission (AIE) reported by our group since 2001 has been developed

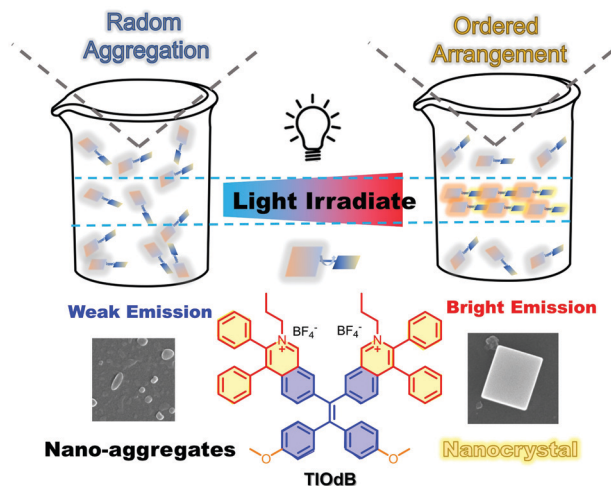
^a AIE Institute, Center for Aggregation-Induced Emission, Key Laboratory of Luminescence from Molecular Aggregates of Guangdong Province, State Key Laboratory of Luminescent Materials and Devices, South China University of Technology, Guangzhou 510640, China. E-mail: wangzhiming@scut.edu.cn

^b Department of Urology, The First Affiliated Hospital of Soochow University, 188 Shizi RD, Suzhou 215006, China

^c HKUST-Shenzhen Research Institute, Shenzhen 518057, China

^d Department of Chemistry, Hong Kong Branch of Chinese National Engineering Research, Centre for Tissue Restoration and Reconstruction, The Hong Kong University of Science and Technology, Clear Water Bay, Kowloon 999077, Hong Kong, China. E-mail: tangbenz@ust.hk

[†] Electronic supplementary information (ESI) available: Synthetic procedures, NMR, spectra, photophysical characterization data, PL spectra, theoretical calculations data, crystal data, cell imaging and cell viability. CCDC 1975683. For ESI and crystallographic data in CIF or other electronic format see DOI: 10.1039/d0mh01200a



Scheme 1 Illustration of the photoexcitation process and molecular structures of TIOdB.

rapidly as an important photophysical behaviour,¹¹ which can be described as weakened emission in benign solvents and intensified with the formation of aggregates in poor solvents. Such AIE luminogens (AIEgens) could overcome the troubling aggregation-caused quenching (ACQ) of conventional luminescent materials,¹² thus expanding the applications of such luminophores in optoelectronic devices, fluorescent bioimaging, disease diagnosis, and therapy.¹³ Hence, developing newer materials based on photophysical processes is of great significance for practical applications.

TIOdB, an isoquinolinium-based organic salt derivative, is prepared to be an ionic-type AIEgen employing the tetraphenylethylene (TPE) framework, as shown in Scheme 1, and its detail characterization is provided in ESI† (Fig. S1–S6). Besides the expected AIE-activity, the fluorescence intensity of TIOdB in organic or aqueous solvents or cells was enhanced under continuous light irradiation, exhibiting an excellent photoactivatable behaviour. Notably, the occurrence of the photoactivation phenomenon is not a photochemical reaction as reported before, but a photophysical-dominant behaviour from aggregation process, as revealed by detailed analysis. Employing measurements of systematic spectra, single crystal, and molecular conformation, a novel mechanism of photoactivation was revealed for the first time, namely photo-induced crystallization with emission enhancement (PICEE). Fortunately, the linear relationship between illumination intensity of source and fluorescence intensity enhancement of TIOdB was observed, which has the potential to optimize the illumination condition of photosynthesis in quantification. In addition, TIOdB is a mitochondrion-targeting fluorescent dye with good biocompatibility, and it exhibits good killing capability towards cancer cells under white light irradiation due to the ROS generation, implying that it can be used as a potential photosensitizer for the PDT process.

Results and discussion

According to our previous reports, the photophysical properties of TIOdB was studied in a mixture of tetrahydrofuran (THF) and

hexane with different fractions (f_H).¹⁴ A weak emission was observed when $f_H = 0\%$, but a strong fluorescence appeared when $f_H = 99\%$, suggesting TIOdB being well soluble in THF but tightly aggregated in the hexane system, which was confirmed by dynamic light scattering (DLS) (Fig. S7A and B in the ESI†). Considering its solubility originating from the ionized framework, water, dimethyl sulfoxide (DMSO) or their mixtures were employed as solvents, and it showed even a weaker emission because of the dominance of the twisted intramolecular charge-transfer (TICT) effect in this process under such circumstances^{6a,b} (Fig. S8A and B in the ESI†). Notably, yellow bright fluorescence in the aqueous solution emerged with the increase in the fluorescence intensity when the irradiation time was prolonged under UV light in air or N₂ condition, as shown in Fig. 1C, exhibiting an impressive fluorescence “turn-on” phenomenon. Comparing to that without irradiation, the fluorescence of TIOdB after 70 min irradiation is much brighter with about 25-fold enhancement (the inset fluorescence photograph in Fig. 1D). In other organic solvents, similar photoactivatable phenomenon also appeared with various degrees of responses, indicating that the difference of solution polarity was not the main factor but the solubility of TIOdB in different solvents might play an important part in the response degree of the fluorescence intensity enhancement (Fig. S9, ESI†). However, the process had become easy in solvents containing the oxygen element

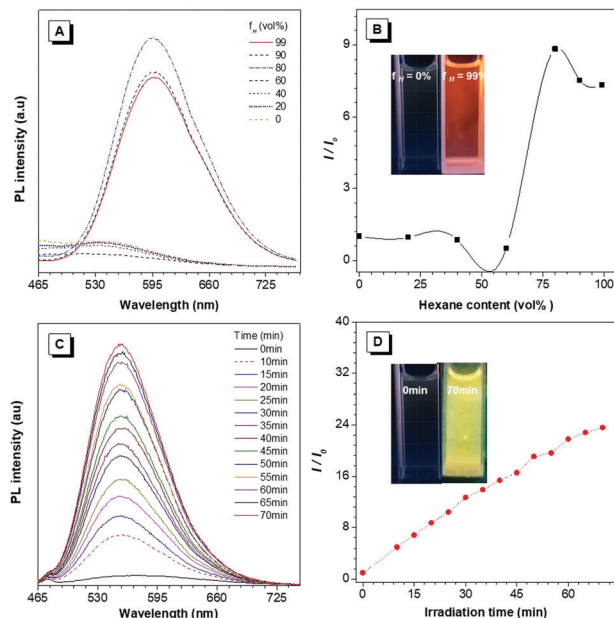


Fig. 1 (A) Photoluminescence (PL) spectra of TIOdB in THF/hexane mixtures with different hexane fractions (f_H) under the same excitation conditions. (B) I/I_0 plots of TIOdB in a mixture of THF/hexane, where I is the intensity with different hexane volume fractions (f_H), and I_0 is the initial intensity in THF. Inset: Fluorescent photos of the THF/hexane mixtures of TIOdB at $f_H = 0$ and 99 vol% taken under 365 nm, 2.48 mW cm⁻² UV light from a hand-held UV lamp. Concentration: 10 μM. (C) Time-dependent PL spectra of TIOdB (10 μM) in aqueous solutions under irradiation of UV light. (D) Plot of the relative fluorescence intensity ($I/I_0@556$ nm) versus different irradiation times. Inset: Fluorescence photographs of solution before and after UV irradiation for 70 min.

(Fig. S9H in the ESI[†]), which might originate from the existence of lone pair electrons in oxygen stabilizing the cationic transition state or intermediate to the photoactive process.

To clearly understand the nature of the photoactivation behavior of TIOdB, the structures before and after light illumination were first investigated *via* the nuclear magnetic resonance (NMR) analysis in the DMSO-*d*₆ solution, in which the location and intensity of proton responses of TIOdB did not change all the time (Fig. 2A). Moreover, by measuring their UV-vis absorption spectra at different irradiation time, we could find that the position of the peaks nearly did not change in Fig. 2B, which was different from the conventional photochemical mechanism for this photoactivation process. However, the intensities decreased gradually by increasing the irradiation time, indicating that the concentration of the sample

solution might reduce gradually, which was possibly caused by the precipitation of big aggregates. Such a change in trend of the absorption intensity was in accord with that of the absorption spectra of a series of diluted TIOdB solutions (Fig. S10 in the ESI[†]). After introducing a low temperature test to freeze molecules with no motion, the PL spectra of TIOdB were measured after UV light irradiation for 30 min at 298 K and 77 K, respectively. As shown in Fig. 2C, the PL intensity at 298 K had enhanced a lot compared to that at 77 K, indicating that the fluorescence improvement of TIOdB depended on the molecular motion to a great extent. Meanwhile, the particle sizes of TIOdB had a clear increasing trend with prolonged light irradiation time in DLS dynamic monitoring (Fig. 2D and Fig. S11A, ESI[†]), and the formation of tighter molecular packing might be the key cause for the fluorescence enhancement. Owing to the ionic characteristics of TIOdB, its electrical conductivity in aqueous solutions, including the large π cationic part and anionic part, was related to the movement ability of molecules or aggregates.¹⁶ Usually, the smaller the aggregate is, the greater the conductivity under the same conditions. As shown in Fig. 2E, its conductivity under different irradiation times decreased by a larger margin than that without light irradiation, which might originate from the increase in the volume of conductive particles with poor movement ability after light irradiation. Obviously, light induced the formation of large aggregates or particles and caused poor migration, which was consistent with DLS results. Taking the above analysis into account, this photoactivation process of TIOdB is a physical behaviour.

To vividly confirm the photoinduced aggregation, the scanning electron microscopy (SEM) was employed for visualizing nanostructure formation and transformation processes. Before light illumination, the nanoparticles were very dispersed with irregular shapes, as shown in Fig. 3A. After irradiation for 30 min (UV-light, 365 nm, 2.48 mW cm⁻²), these scattered nanoparticles became tighter and the nano-block crystals appeared, as shown in Fig. 3B. Prolonging the irradiation time to 60 min, the large-scale emergence of nano-block crystals with larger sizes is observed, as shown in Fig. 3C, whose emission was also enhanced sharply. As a comparison, the SEM images of the TIOdB aqueous solution, which is allowed to stand for 60 min, were also collected, and there were no nano-block crystals observed, but nanoparticles with irregular shapes appeared, as shown in Fig. 3D, indicating that light plays an important role in the process of nanocrystal formation. The crystalline characteristics of the nanocrystals were further verified by X-ray diffraction (XRD), and the clear crystalline peaks of the TIOdB sample after light illumination for 60 min appeared as compared to that before light illumination (Fig. S12A in the ESI[†]). All these results reveal that the photo-induced crystallization process would become the main factor for its fluorescence enhancement. Alternatively, the light illumination makes random TIOdB molecules crystallize more clearly and efficiently. Interestingly, this photoactivation behavior must be occurring in organic or aqueous solution so that the single molecule or loose aggregates could easily complete the process of conformational adjustment and migration for crystallization owing to its double ionized framework. In contrast, such changes became so hard that no

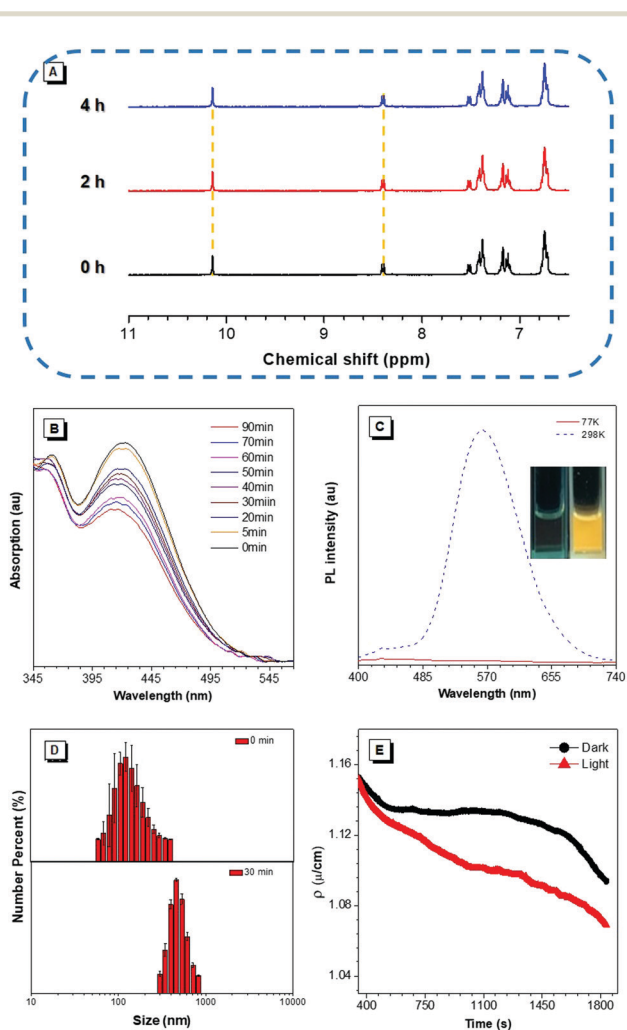


Fig. 2 (A) Change of ¹H NMR spectra of TIOdB in the DMSO-*d*₆ solution (2×10^{-3} M) before and after 365 nm, 2.48 mW cm⁻² UV light from a hand-held UV lamp for 0, 2 h, and 4 h. (B) UV spectra of TIOdB (10 μ M) in the DMSO solution irradiated with 365 nm, 2.48 mW cm⁻² UV light from a hand-held UV lamp for different times. (C) PL spectra of TIOdB (10 μ M) in the DMSO solution after irradiation with 365 nm, 2.48 mW cm⁻² UV light from a hand-held UV lamp for 30 min at 77 and 298 K respectively. (D) DLS results before and after irradiation for 10 min in aqueous solutions. (E) The conductivity of TIOdB in aqueous solutions with different light illumination time and in dark condition. Concentration: 10 μ M.

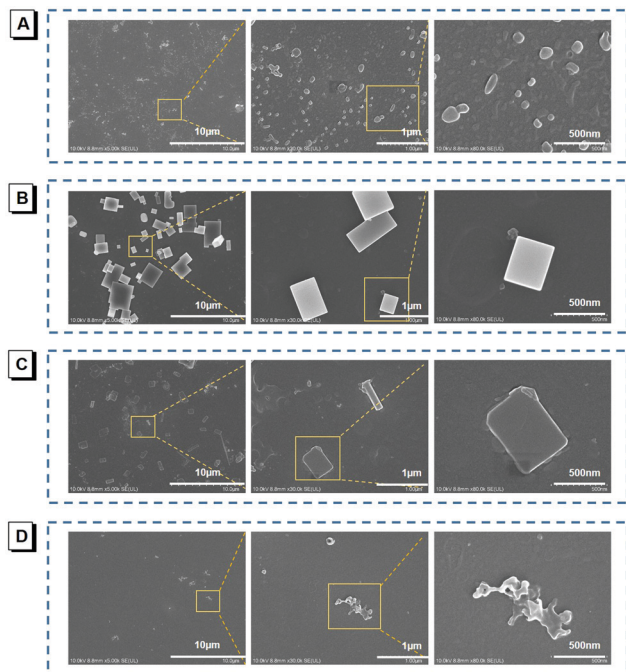


Fig. 3 Time-dependent SEM images to visualize the aggregation processes and the change in the aggregation morphology of the TiO₂B aqueous solution (A) before irradiation; after irradiation for (B) 30 min and (C) 60 min respectively; (D) SEM images of TiO₂B aqueous, which is allowed to stand for 60 min as a control group. Concentration: 10 μM.

obvious fluorescence enhancement was observed in crystal or powder. The photoactivation process of TiO₂B is not a chemical but a physical behaviour. Notably, we report here for the first time that light could induce the formation of nanocrystals.

To explore the driving forces of PICEE, a theoretical simulation was carried out to describe the change in the molecular conformation of TiO₂B in the DMSO solvent. The large geometric change occurred between the ground state (S_0) and the lowest energy-excited state (S_1) (Fig. S13E and F, ESI[†]). The conformation of S_1 became more planar than that of S_0 , whose torsion angles changed from 48.02°, 39.65°, 44.11°, and 44.21° to 39.02°, 36.74°, 31.72°, and 42.72°, which is more favourable for generating intermolecular interactions in the photo-generated excited state, such as more intermolecular π - π , C-H \cdots π and C-O \cdots H interactions facilitate the self-assembled arrangement and formation of nano-crystals. Analysing the single crystal of TiO₂B obtained from the evaporation of dichloromethane/petroleum ether mixtures, the multiple intermolecular C-H \cdots π and C-O \cdots H interactions were observed (Fig. S13A-D, ESI[†]), which were beneficial to rigidify the molecular conformation and restrict the intramolecular motions to a greater extent. Moreover, the anion was bound in a fixed position. On the one hand, the negative charge would well balance the quenching effect of cations on the luminescent centre, and on the other hand, the formation of the F \cdots H bond further restricted the molecular movement. All of these effects were beneficial to the luminescence enhancement.

To better elucidate the realistic application of PICEE, the emission intensity of TiO₂B in the H₂O solution under different light illumination intensities was monitored, and a good linear



Fig. 4 (A) Fluorescence emission spectra of TiO₂B (10 μM) in the H₂O solution towards white light of different intensities. (B) Plot of the fluorescence intensity enhancement with TiO₂B (10 μM) against white light intensity, where I is the intensity with illumination of white light of different intensities, and I_0 is the initial intensity with illumination of 1 mW cm⁻² white light. Y is the I/I_0 and X is the light intensity; (C) simulative schematic of getting the optimum light conditions of greenhouse vegetable; (D) photoactivation behavior in HeLa cells recorded by confocal laser scanning microscopy. HeLa cells were stained with TiO₂B (1 μM) for 15 min. Scale bar: 20 μm.

relationship between the fluorescent intensity enhancement and irradiation intensity was found, as shown in Fig. 4A and B, which could be used as an auxiliary means to optimize the photosynthesis intensity and guide the growth condition for plants. As shown in Fig. 4C, as a control, a monitor containing the TiO₂B aqueous solution was placed near vegetables at the same height under the same illumination intensity. Consequently, we could observe the growth of vegetables and what the illumination intensity is the most beneficial one for the vegetable growth can be obtained by the fluorescence change. So, TiO₂B could work as a potential candidate to get the optimum illumination conditions of greenhouse vegetables.

Moreover, inspired by TPE-IQ derivatives being used as organelle-targeting probes,^{14,15} the cell imaging performance of TiO₂B was investigated. After incubation with irradiation for 15 min, a light-up fluorescence was observed inside cells, and almost no emission was detected outside cells even without washing, implying that the photoactivation behaviour of TiO₂B was kept and the simpler operation was adopted in practical applications (Fig. 4D). Co-staining with the commercial dyes of MTR, TiO₂B exhibited high mitochondria-targeting with more clear fluorescence imaging in dot or linear reticulum-like structures when increasing Z-axis (Fig. S15A and S16, ESI[†]),

which could really reflect the mitochondrial distribution with the high-fidelity spatial temporal feedback.¹⁷ In addition, the effect of the photodynamic therapy (PDT) worked very well because of mitochondria-targeting and its efficient generation of reactive oxygen species (ROS) upon white light irradiation (Fig. S15B and C, ESI†).¹⁵ Employing the theoretical energy level analysis of TIOdB, the highly separated charge distribution was observed from natural transition orbitals (NTOs) (Fig. S14B, ESI†), whose hole was mainly localized on TPE moieties and particle was predominantly centered at the isoquinolinium core, and these distributions contributed to the lowering of the conversion barrier between the singlet and triplet states.¹⁸ Simultaneously, the energy gap between S_1 and T_3 states was only 0.10 eV, which was beneficial for the triplet exciton generation (Fig. S14A, ESI†).

Conclusions

In summary, we developed a new photoactivatable fluorophore, named as TIOdB, which exhibited an excellent photoactivation property inside and outside the cell under a new photoactivatable mechanism of photo-induced crystallization with emission enhancement (PICEE). Such a physical process can be interpreted as the change in the molecular conformation in the excited state of TIOdB, a change that leads to self-assembling into a regular arrangement. As a result, nanocrystals or larger aggregates were formed by intermolecular strong interactions under light excitation. The linear relationship between the illumination intensity and fluorescence intensity enhancement can be a candidate in optimizing the plant growth conditions because the photosynthesis of plant growth has certain tolerance towards light intensity. In addition, TIOdB holds a potential in high-quality bioimaging and therapy with good biocompatibility. Such intriguing results indicate that it can provide a new general strategy for the formation of nanocrystals and the development of more diverse functional materials with a new photoactivatable mechanism.

Conflicts of interest

There are no conflicts to declare.

Acknowledgements

The authors are grateful for financial support from the National Natural Science Foundation of China (21788102, 51673118 and 201975077), The National Key R&D Program of China (Inter-governmental cooperation project, 2017YFE0132200), Innovation and Technology Commission of Hong Kong (ITC-CNERC14SC01), Fundamental Research Funds for the Central Universities (2019ZD04), and Fund of Key Laboratory of Luminescence from Molecular Aggregates of Guangdong Province (2019B030301003).

Notes and references

- (a) T. P. Yoon, M. A. Ischay and J. Du, *Nat. Chem.*, 2010, **2**, 527; (b) S. Kwak, J. P. Giraldo, M. H. Wong, V. B. Koman, T. T. S. Lew, J. Ell, M. C. Weidman, R. M. Sinclair, M. P. Landry, W. A. Tisdale and M. S. Strano, *Nano Lett.*, 2017, **17**, 7951.
- (a) O. Warburg, *Science*, 1958, **128**, 68; (b) D. Gust, T. A. Moore and A. L. Moore, *Acc. Chem. Res.*, 2009, **42**, 1890.
- (a) Z. Li, X. Li, H. Chen, C. He, L. Wang, Y. Yang, S. Wang, H. Guo and S. H. Liu, *Dyes Pigm.*, 2019, **162**, 712; (b) L. Wang and Q. Li, *Chem. Soc. Rev.*, 2018, **47**, 1044; (c) S. Yang, J. Liu, Z. Cao, M. Li, Q. Luo and D. Qu, *Dyes Pigm.*, 2018, **148**, 341.
- (a) C. C. Ko and V. W. W. Yam, *Acc. Chem. Res.*, 2018, **51**, 149; (b) L. Dong, Y. Feng, L. Wang and W. Feng, *Chem. Soc. Rev.*, 2018, **47**, 7339.
- A. S. Lubbe, W. Szymanski and B. L. Feringa, *Chem. Soc. Rev.*, 2017, **46**, 1052.
- (a) X. Gu, E. Zhao, J. W. Y. Lam, Q. Peng, Y. Xie, Y. Zhang, K. S. Wong, H. H. Y. Sung, I. D. Williams and B. Z. Tang, *Adv. Mater.*, 2015, **27**, 7093; (b) X. Gu, E. Zhao, T. Zhao, M. Kang, C. Gui, J. W. Y. Lam, S. Du, M. M. T. Loy and B. Z. Tang, *Adv. Mater.*, 2016, **28**, 5064; (c) S. Li, X. Ling, Y. Lin, A. Qin, M. Gao and B. Z. Tang, *Chem. Sci.*, 2018, **9**, 5730; (d) Z. Ye, H. Yu, W. Yang, Y. Zheng, N. Li, H. Bian, Z. Wang, Q. Liu, Y. Song, M. Zhang and Y. Xiao, *J. Am. Chem. Soc.*, 2019, **141**, 6527.
- (a) M. Li, J. Zhao, H. Chu, Y. Mi, Z. Zhou, Z. Di, M. Zhao and L. Li, *Adv. Mater.*, 2019, **31**, 1804745; (b) M. Karimi, P. S. Zangabad, S. Baghaee-Ravari, M. Ghazadeh, H. Mirshekari and M. R. Hamblin, *J. Am. Chem. Soc.*, 2017, **139**, 4584.
- (a) X. Jia, C. Shao, X. Bai, Q. Zhou, B. Wu, L. Wang, B. Yue, H. Zhu and L. Zhu, *Proc. Natl. Acad. Sci. U. S. A.*, 2019, **116**, 4816; (b) R. Kadono, R. M. Macrae and K. Nagamine, *Phys. Rev. B: Condens. Matter Mater. Phys.*, 2003, **68**, 2452042A.
- (a) B. Yoon, S. Lee and J. M. Kim, *Chem. Soc. Rev.*, 2009, **38**, 1958; (b) D. Kitagawa, H. Nishi and S. Kobatake, *Angew. Chem., Int. Ed.*, 2013, **52**, 9320.
- (a) J. F. Stoddart, *Angew. Chem., Int. Ed.*, 2017, **56**, 11094; (b) C. Petermayer and H. Dube, *Acc. Chem. Res.*, 2018, **51**, 1153; (c) S. J. Wezenberg and B. L. Feringa, *Nat. Commun.*, 2018, **9**, 1984.
- J. Luo, Z. Xie, J. W. Y. Lam, L. Cheng, B. Z. Tang, H. Chen, C. Qiu, H. S. Kwok, X. Zhan, Y. Liu and D. Zhu, *Chem. Commun.*, 2001, 1740.
- (a) Y. Wang, Y. Chen, H. Wang, Y. Cheng and X. Zhao, *Anal. Chem.*, 2015, **87**, 5046; (b) B. Andreiuk, A. Reisch, E. Bernhardt and A. S. Klymchenko, *Chem. – Asian J.*, 2019, **14**, 836.
- (a) A. Shao, Y. Xie, S. Zhu, Z. Guo, S. Zhu, J. Guo, P. Shi, T. D. James, H. Tian and W. H. Zhu, *Angew. Chem., Int. Ed.*, 2015, **54**, 7275; (b) J. Mei, N. L. Leung, R. T. Kwok, J. W. Lam and B. Z. Tang, *Chem. Rev.*, 2015, **115**, 11718.
- C. Gui, E. Zhao, R. T. Kwok, A. C. Leung, J. W. Lam, M. Jiang, H. Deng, Y. Cai, W. Zhang, H. Su and B. Z. Tang, *Chem. Sci.*, 2017, **8**, 1822.
- (a) E. G. Zhao, H. Q. Deng, S. J. Chen, Y. N. Hong, C. W. T. Leung, J. W. Y. Lam and B. Z. Tang, *Chem. Commun.*, 2014, **50**, 14451; (b) M. Jiang, X. Gu, R. T. Kwok, Y. Li, H. H. Sung, X. Zheng, Y. Zhang, J. W. Lam, I. D. Williams, X. Huang, K. S. Wong and B. Z. Tang, *Adv. Funct. Mater.*, 2018, **28**, 1704589; (c) K. Chen, R. Zhang, Z. Wang, W. Zhang and B. Z. Tang, *Adv. Opt. Mater.*, 2019, 1901433.

- 16 (a) J. Wang, X. Gu, P. Zhang, X. Huang, X. Zheng, M. Chen, H. Feng, R. T. K. Kwok, J. W. Y. Lam and B. Z. Tang, *J. Am. Chem. Soc.*, 2017, **139**, 16974; (b) W. Wang, R. Balasubramanian and R. W. Murray, *J. Phys. Chem. C*, 2008, **112**, 18207.
- 17 (a) J. Zhang, Q. Wang, Z. Guo, S. Zhang, C. Yan, H. Tian and W. H. Zhu, *Adv. Funct. Mater.*, 2019, **29**, 1808153; (b) Q. Hu, M. Gao, G. Feng and B. Liu, *Angew. Chem., Int. Ed.*, 2014, **53**, 14225.
- 18 (a) H. Uoyama, K. Goushi, K. Shizu, H. Nomura and C. Adachi, *Nature*, 2012, **492**, 234; (b) K. Schmidt, S. Brovelli, V. Coropceanu, D. Beljonne, J. Cornil, C. Bazzini, T. Caronna, R. Tubino, F. Meinardi, Z. Shuai and J.-L. Brdas, *J. Phys. Chem. A*, 2007, **111**, 10490.